IRAQI BULLETIN OF GEOLOGY AND MINING (IBGM)\
IRAQ GEOLOGICAL SURVEY (GEOSURV-IRAQ)

*IBGM (**2025**, Vol 21; Issue 1)* *121-133*

SEISMIC EXPRESSION OF KARST-RELATED FEATURES AND 3D SEISMIC EVIDENCE OF THE EFFECTS OF CARBONATE KARST COLLAPSE AND FAULT SYSTEM ON HYDROCARBON MIGRATION PATH IN MERJAN-WEST KIFL OIL FIELDS, CENTER OF IRAQ

Ali M. Al-Rahim[1], and Mohammed Sadi Fadhel[2]

[1] University of Baghdad, College of Science, Department of Geology, Baghdad – Iraq, e-mail: ali.m@sc.uobaghdad.edu.iq; alial_rahim@yahoo.com
[2] Oil Exploration Company, Iraq, e-mail: mohammedal_hamdani@yahoo.co.uk
*****Corresponding author e-mail: ali.m@sc.uobaghdad.edu.iq*

Type of the Paper (Article)
Received: 02/ 08/ 2024
Accepted: 05/ 01/ 2025
Available online: 27/ 06/ 2025

Abstract

A seismic study of 2D/3D data Volume of Merjan-West Kifl oil fields, in central Iraq, was conducted to delineate karst features and fault systems in the area and their role in hydrocarbon migration. 3D Seismic data depict karst features and faults that act as a pathway to migrate hydrocarbons from Late Jurassic source rocks (Sargelue and Sulaiy formations) to the Early Cretaceous reservoir rocks (Hartha, Sadi, Nahr Umr, and Zubair formations) in the area. Most of the Cretaceous carbonate formations, such as Yamama, Shuaiba, and Mishrif in the area, have undergone chemical erosion after deposition and diagenesis, generating karst features. Their surfaces appear as irregular depressions at erosion or collapse of deeper karst hole locations. The seismic reflection image below the karst feature is poor because they have significantly slower velocities than the surrounding sediments. Consequently, high contrast in acoustic impedance occurs, and the seismic reflection signature is distinctive as a Gull-winged depression in cross-section. This was permitted to delineate and map the karst in the area. The size of these karsts is usually a few meters to a few hundred. Delineation of the karst features was attempted utilizing seismic attributes mapping using a variance cube. Seismic attributes were applied to confirm the physical properties and behavior of karsts. They were illustrated with low frequency and high reflection magnitude.

Keywords: Merjan-West Kifl oil fields; Karst and caves; Seismic attribute; Gull-winged depression; Reflection strength; Variance attribute; Migrate hydrocarbons; Fault system; Carbonate karst.

1. Introduction

Karst is a good example of the chemical weathering the rocks. Through the dissolution of rocks, landscapes are formed, such as limestone caves, where most karst develops in carbonate rocks

ISSN 1811-4539, EISSN 3005-3714
https://doi.org/10.59150/ibgm2101a08
IBGM: http://ibgm-iq.org/
Academic Scientific Journals: www.iasj.net

and gypsum. They form slowly in dry climates but faster in humid climates. Karst forms large pathways for rapid groundwater flow in cave networks depending on stratigraphy, faulting, and jointing. Karst features are developed on carbonate platforms where the rivers that meander toward the shelf break during times of lowered sea level often incise attached carbonate ramps and shelves (Esker et al., 1998). Because it may affect the production and presence of hydrocarbons, karst is a significant feature. Finding and defining these characteristics will be essential to the resource's assessment (Bown, 2011; Fisher et al., 2020). There is a dearth of literature on imaging buried karst structures. The majority of the literature addresses the practical challenges of identifying karst features, especially possible sinkholes or near-surface caverns (Waltham & Fookes, 2003). Discrimination and mapping of karst features are very important not only for reserve stimulation but also to avoid potential risks during the drilling. Also, they play an important role in the migration of fluids such as lice hydrocarbon. In their seismic time structural map, Rafaelsen et al., (2008) were able to provide compelling proof of sinkhole growth (Figure 1). Zuo et al., (2009) use the discontinuous deformation analysis (DDA) method for 3D seismic data to calculate the deformation field and analyze the subsidence mechanism and deformation field of a karst collapse column at Xieqiao, in the south of China. Burberry et al., (2016) use time-migrated 2D seismic reflection data to determine the distribution, scale, and genesis of karst in a 3 Km thick, Jurassic – Miocene carbonate-dominated succession in the Persian Gulf. They map 43 seismic-scale karst features, which are expressed as vertical pipe columns of chaotic reflections capped by downward-deflected depressions that are lapped by overlying strata. Karst-induced characteristics in the Boonville area of North Central Texas are defined by Singh et al. (2010) using "Amplitude, Instantaneous Phase, Trace Envelope and Dip of Maximum Similarity" attributes. They show that these seismic attributes can be creatively utilized to achieve interpretational objectives beyond those from only conventional seismic data.

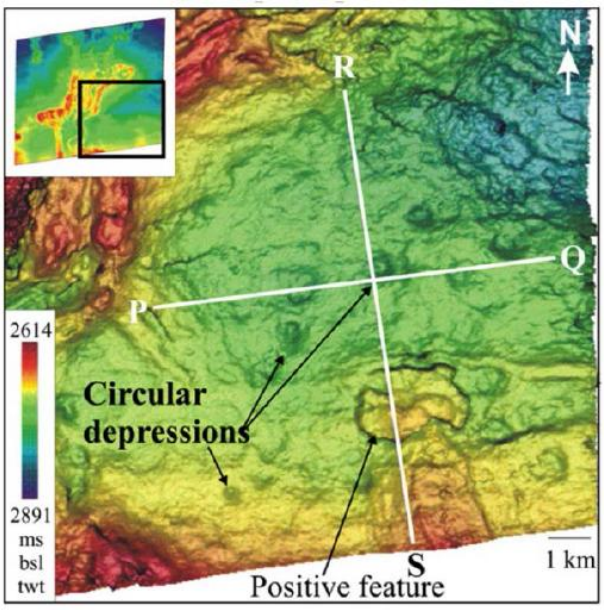

Figure 1. Time structure map at the Top Evaporates horizon displaying circular depressions interpreted as sinkholes (Rafaelsen et al., 2008).

Karst systems' natural abrupt lateral changes in physical characteristics produce a lot of geophysical noise, which makes it difficult to filter and interpret traditional seismic signals. Ebuna et al., (2018) developed a semi-automated technique for determining and approximating the structural boundaries of karst systems by applying neural networks to multi-attribute seismic interpretation.

The current research is a seismic interpretation of 2D/3D seismic data available in the Oil Exploration Company for the Merjan-West Kifl oil fields. It is an attempt to understand the role of karst features in hydrocarbon migration from source to reservoir rocks in the fields.

The Merjan-West Kifl Oil fields are located in the middle of Iraq, west of the Euphrates River, within Al-Najaf – Karbala province, approximately 60 – 70 Km to the southeast of Baghdad (Figure 2a).

Between the Stable Platform to the west and the Mesopotamian Basin, the Merjan region is situated at a crucial location (Figure 2b). The Oil Exploration Company conducted the 3D survey, and as the initial amplitude gain was maintained, the processing sequence was created to make structural interpretation more dependable and straightforward. The Merjan-West Kifl Oil fields are covered by 3D seismic data covering 1026.17 km² operation regions.

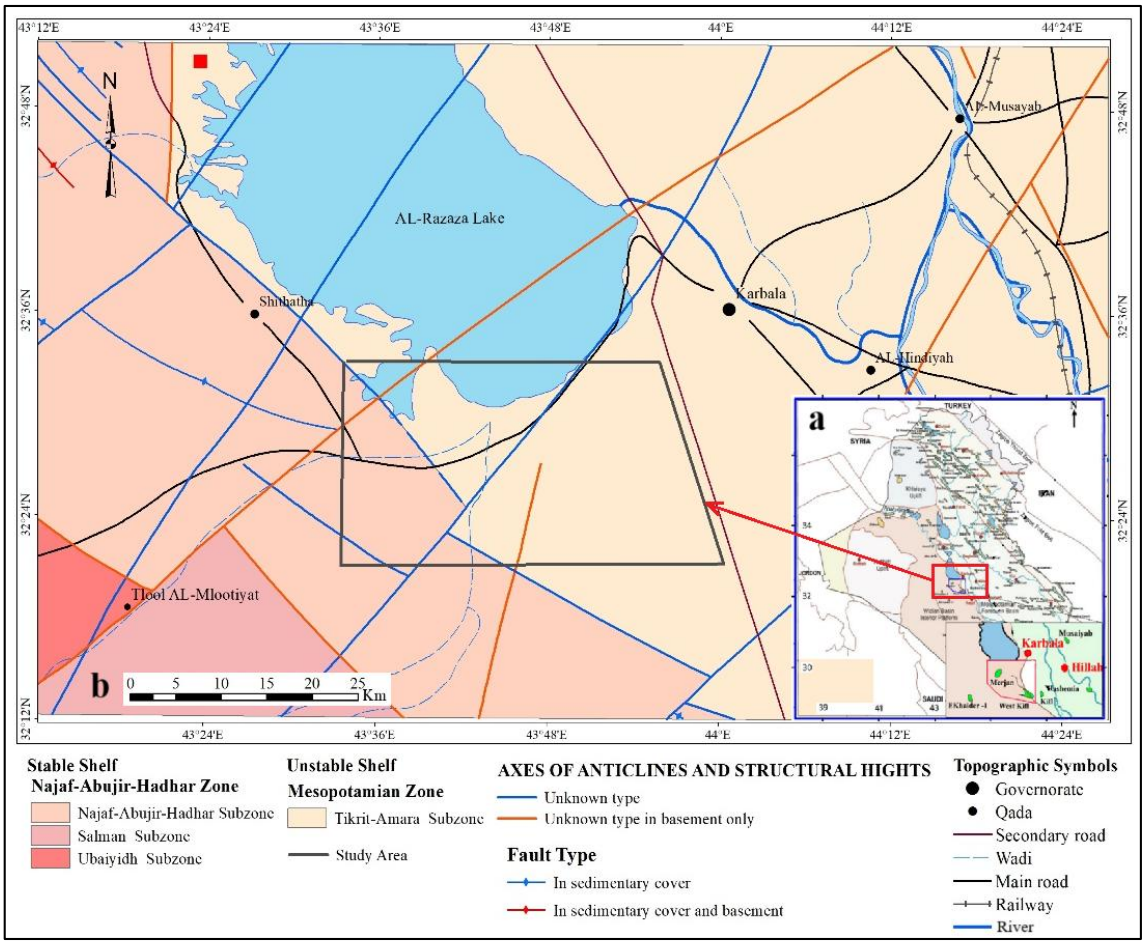

Figure 2. a) Location map (after Al-Ameri et al., 2015). b) Tectonic map of a study area (after Al-Kadhimi, et al., 1996).

2. Methodology

Depression features due to dissolution, such as sinkholes and karst collapse, are equally common in carbonate environments. The seismic signature of the irregular shape and distribution of these features is chaotic reflection, which makes it hard to image them precisely (Eberli et al., 2005).

The methodology of work includes four steps in our paper: (1) horizon and fault picking (2) karst or cave indicator in seismic section (3) karst expression in variance attributes slices (4) the karst feature analogues. Horizon definitions were made depending on synthetic seismograms of Me-1 and Wkf-1 well data. Picking horizons is the next step in the interpretation work on the area. Seismic data have more information that can be extracted to delineate structural and stratigraphic features. The focus was mainly on the study of karst or cave features. Also, fault picking was conducted in the area.

2.1. Criteria for recognizing caves in the seismic sections

1. Irregular reflections in complex karst, consequently, phase changes and amplitude discontinuities along reflections. The abrupt change in lithology from wall rock to cavern results in abrupt changes in impedance and seismic amplitudes.

2. Depression in seismic cross-section is gull-wing shaped. This shape results from increasing sag intensity and dip as one moves toward the cave core.

3. Vertically-aligned features.

4. The larger cave complexes are long-lived, exhibiting several levels of cave collapse. Concave-up sinkhole reflections or irregular hummocky reflection configurations directly indicate negative karst features (Moldovanyi et al., 1995). The karstification patterns vary widely, from pervasive with large karst holes to more localized with a dendritic pattern or even a drainage pattern (Vahrenkamp et al., 2005).

2.2. The karst feature analogues

The reference to data is becoming mandatory for successful work. Analogs have been elucidated by seismic section and variance slice. An example is from the Minagish oil field in Kuwait (El-Emam et al., 2013) to clarify our caves of interest (Figures 3 and 4).

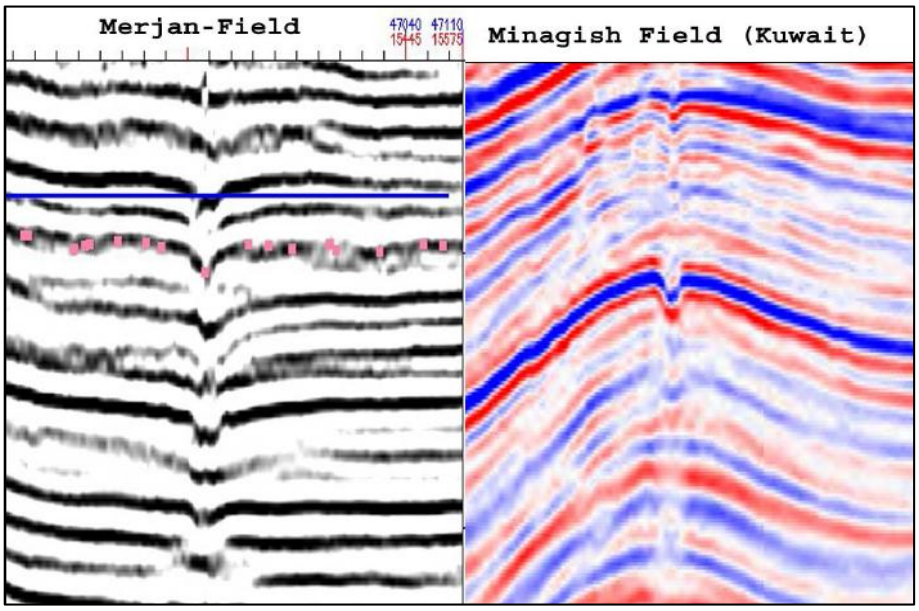

Figure 3. A comparison of two caves as seen in the seismic section; the left from the Merjan field (Iraq) and the right from the Minagish, Kuwait (El-Emam et al., 2013), where both have expression in seismic cross-section as gull-wing shape.

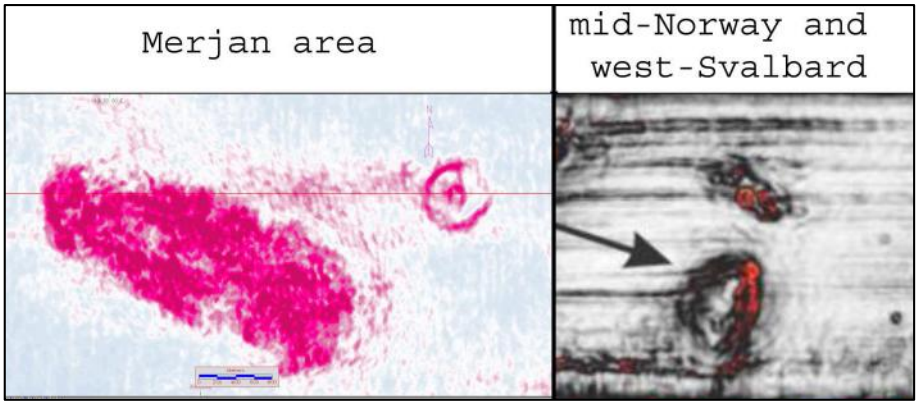

Figure 4. A comparison of two caves as seen in seismic variance attribute. The left from the Merjan field (Iraq) and the right from the mid-Norway and west-Svalbard (Virs, 2015).

3. Results

3.1. Karst Delineation and Hydrocarbon leakage

Since porous karst systems house up to 50% of the world's hydrocarbon reserves, karst research is regarded as being of utmost relevance in petroleum geology (Ford, 2007). A study of vertical sections of 3D seismic data detected the presence of cave features in the study area. These features and faults can act as pathways for transporting the hydrocarbon from the source to the reservoir rocks. They enhance the permeability system in the Early Cretaceous carbonate formations such as Yamama, Mishrif, and Hartha, in the field.

Determination of these features requires processing the seismic cube into the variance attribute cube. This process helped to identify the distribution of karst zones in the temporal and spatial dimensions. Several karsts were determined in the area and reached 35 features in different locations and at several levels with different dimensions; they were referred to with numbers. Figure 5 shows the distribution of 37 karst features which are delineated in the interested area. Details of these features are inserted in Table 1.

The information in the table represents the results of interpretation works, which were based on checking the seismic data from trace to trace and horizontal variance sections. Thus, fault systems were interpreted in the area to help in understanding the development of the karst with time (Figure 6). The faults play an important role in the continuity of liquid movement and form the net system of active channels that pass the fluids through the stratigraphic column in the area.

One of the most important indicators of hydrocarbon leakage from source rocks into several locations within sedimentary succession across these channels and faults is the presence of bitumen in the newly drilled water well in the area, which is Wc-1 (Bottom right in Figure 6). The figure also shows fault systems that were picked and projected on regional faults from the tectonic map of Iraq, karst features, and water wells.

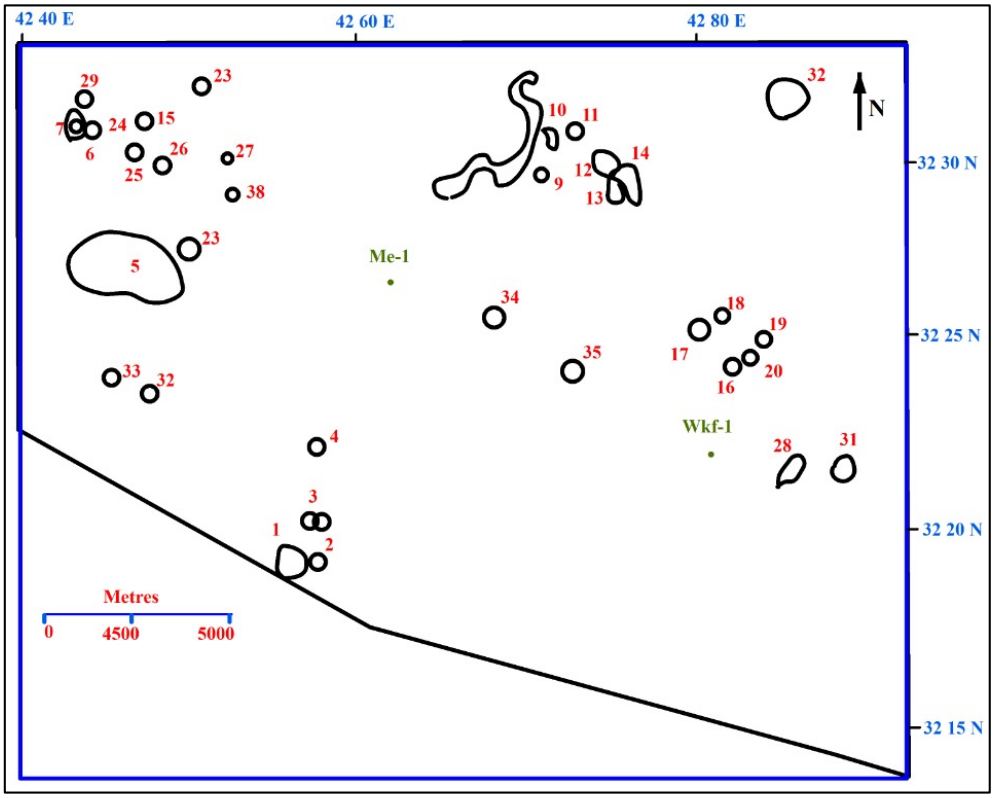

Figure 5. Karst features distribution in the Merjan oil field area. Me-1 and Wkf-1 are the locations of the Merjan and West Kifl wells in the study area.

Table 1. Karst Number, time interval, Formations affected by chemical weathering, and diameters of the karst features.

Karst Number	Time range (ms)	Geological Formation	Diameter of karst zone (m)
1 a, b	100 – 500	Safawi to surface	999
2	200 – 350	Safawi to Hartha	385
3	200 – 350	Safawi to surface	660
4	200 – 350	Safawi to Hartha	475
5	100 – 1200	Sargelue to Quaternary succession	5221
6	300 – 1200	Sargelue to Hartha	357
7	300 – 1200	Sargelue to Hartha	285
8	300 – 630	Rumaila to Hartha	296
9	300 – 630	Rumaila to Hartha	285
10	300 – 630	Rumaila to Hartha	420
11	300 – 630	Rumaila to Hartha	450
12	300 – 630	Rumaila to Hartha	598
13	300 – 630	Rumaila to Hartha	756
14	300 – 630	Rumaila to Hartha	740
15	200 – 850	Rumaila to Hartha	600
16	200 – 850	Rumaila to Hartha	200
17	200 – 850	Sadi to Hartha	600
18	200 – 850	Rumaila to Hartha	480
19	200 – 850	Rumaila to Hartha	387
20	200 – 850	Rumaila to Hartha	100
21	150 – 500	Hartha to Quaternary succession	555
23	300 – 1200	Sargelue to Hartha	950
24	500 – 1100	Sargelue to Hartha	263
25	500 – 1100	Sargelue to Hartha	460
26	500 – 1100	Sargelue to Hartha	273
27	500 – 1100	Sargelue to Hartha	330
28	300 – 1100	Sargelue to Hartha	700
29	500 – 1100	Sargelue to Hartha	416
30	500 – 1100	Sargelue to Hartha	285
31	300 – 1200	Sargelue to Hartha	623
32	450 – 1200	Sargelue to Hartha	631
33	450 – 1200	Sargelue to Hartha	328
34	875 – 1200	Sargelue to Nahr Umr	990
36	600 – 1200	Sargelue to Nahr Umr	725
37	300 – 1200	Sargelue to Hartha	112

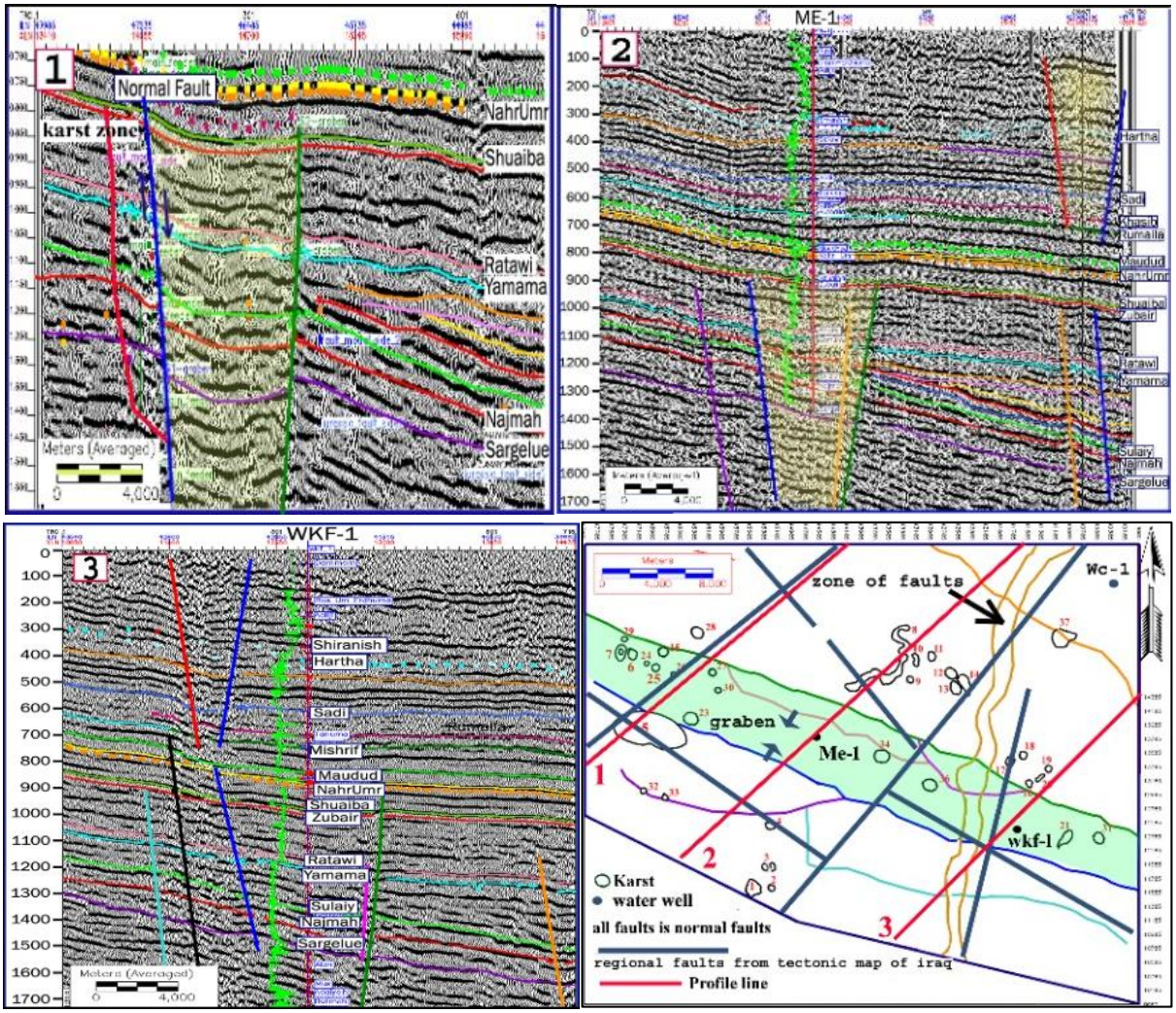

Figure 6. 1, 2, and 3 are seismic sections that illustrate the picked fault system in the area. The bottom right part of the figure delineated karst features, which are posted on the same map of the oil field area with picked fault system and regional faults from the tectonic map of Iraq. See the location of the Wc-1 well in the upper right corner.

Subfigures 7a to 7h show examples of the depicted karst features on the seismic sections for the study area with their locations.

One of the most effective tools for karst mapping is 3D visualization. It allows the interpreter to view the 3D cube from various angles and/or in various ways. A 3D representation of some karst that was seen in the field is shown in Figure 8.

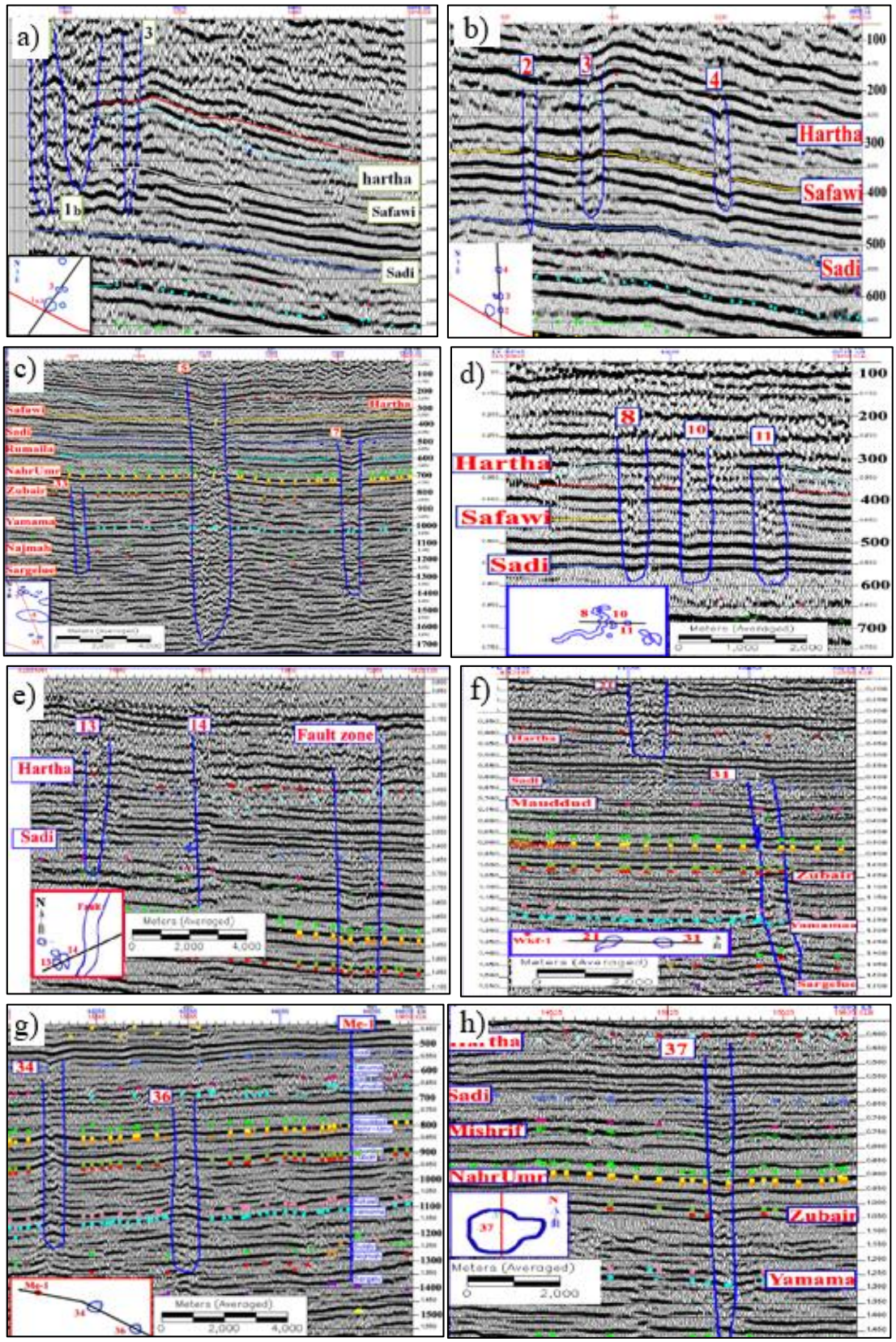

Figure 7. An arbitrary seismic section passes through karst no. a) 1a, b, and 3 features. b) 2, 3, and 4 features. c) 33, 5, and 7 features. d) 8, 10, and 11 features. e) 13, 14 features and fault zone. f) 21, and 31 features. g) 36, and 34 features h) 37 features, respectively.

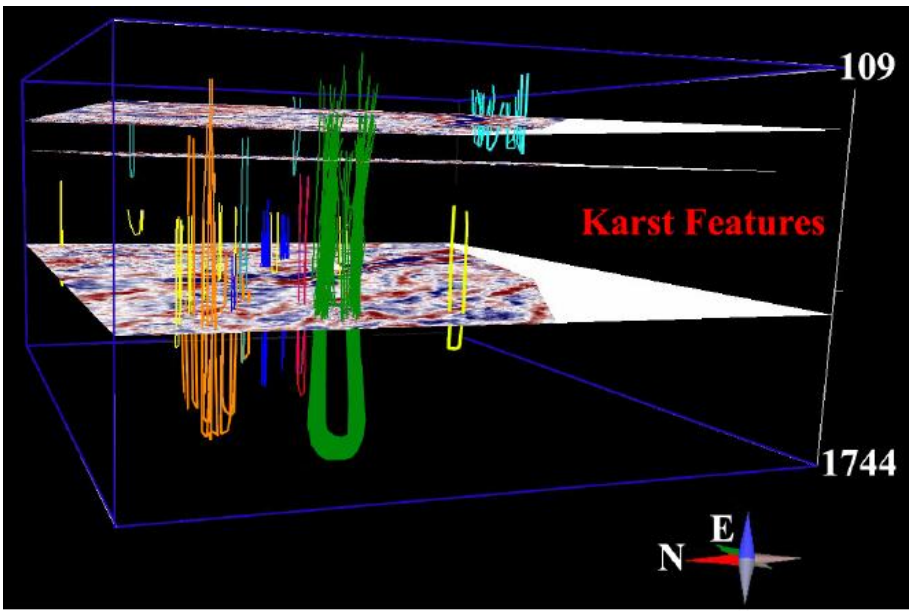

Figure 8. Perspective 3D view of the karst features. Some karsts are extended to deep source formations, while others are restricted along the shallow formations. See Table 1 for more details.

3.2. Seismic Attributes

The 3D seismic data volume of the Merjan field was processed to calculate seismic attributes. Variance, Instantaneous frequency, reflection magnitude, and instantaneous phase were computed.

3.2.1. Seismic variance attributes

Spatial modeling of karst is applied using variance attributes. The original three-dimensional reflectivity data was converted into a variance cube. This cube illustrates the discontinuities in the horizontal continuity of amplitude and is obtained from the assessment of local variation in the signal. This cube was often utilized during the interpretation process for both cave discrimination and fault interpretation. They have been provided with effective tools for distinguishing karst due to the obvious change in amplitude behavior through the karst (Figure 9).

3.2.2. Instantaneous frequency, phase, and reflection magnitude

Instantaneous frequency sections show low-frequency values along the karst feature. Figure 10 shows examples of these characters. The reflection magnitude attribute and instantaneous phase were constructed. They explain the lateral variation at the karst location. High reflection magnitudes are seen at cave locations. The instantaneous phase reflects the clear change in phase beginning at the edges of karst features.

The behavior of seismic attributes is attributed to the physical properties of the cave zone. The

decrease of average density through complex cave systems. The decrease in density is due to the presence of fluid and porous systems. Also, this will lead to a decrease in the seismic velocity through the karst features.

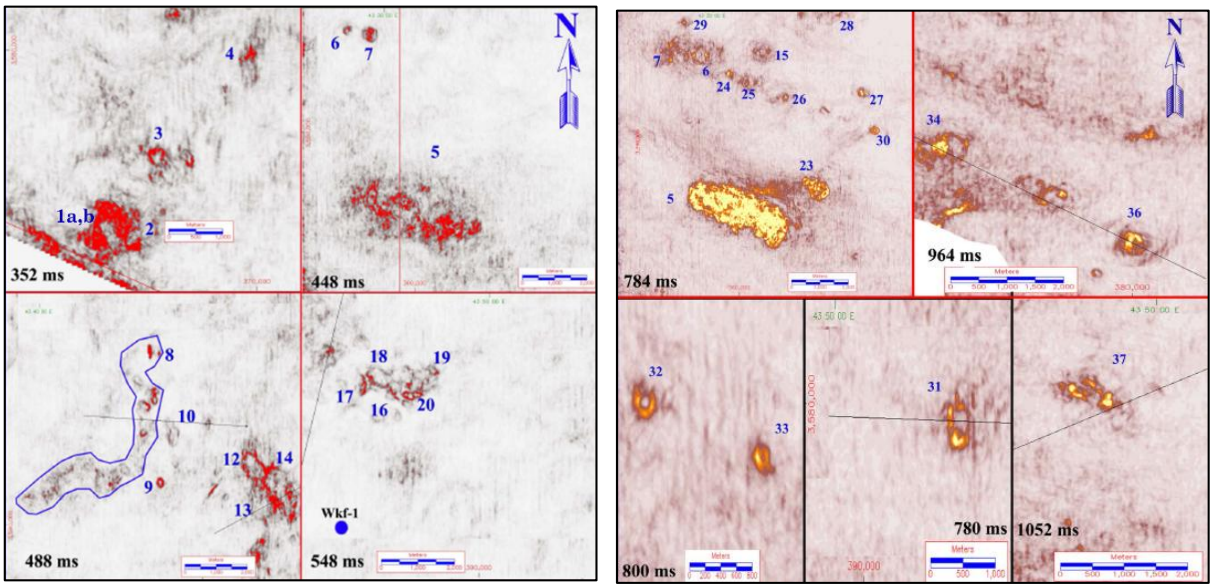

Figure 9. Variance slices at different levels, show the karst features. See details for each feature number in Table 1.

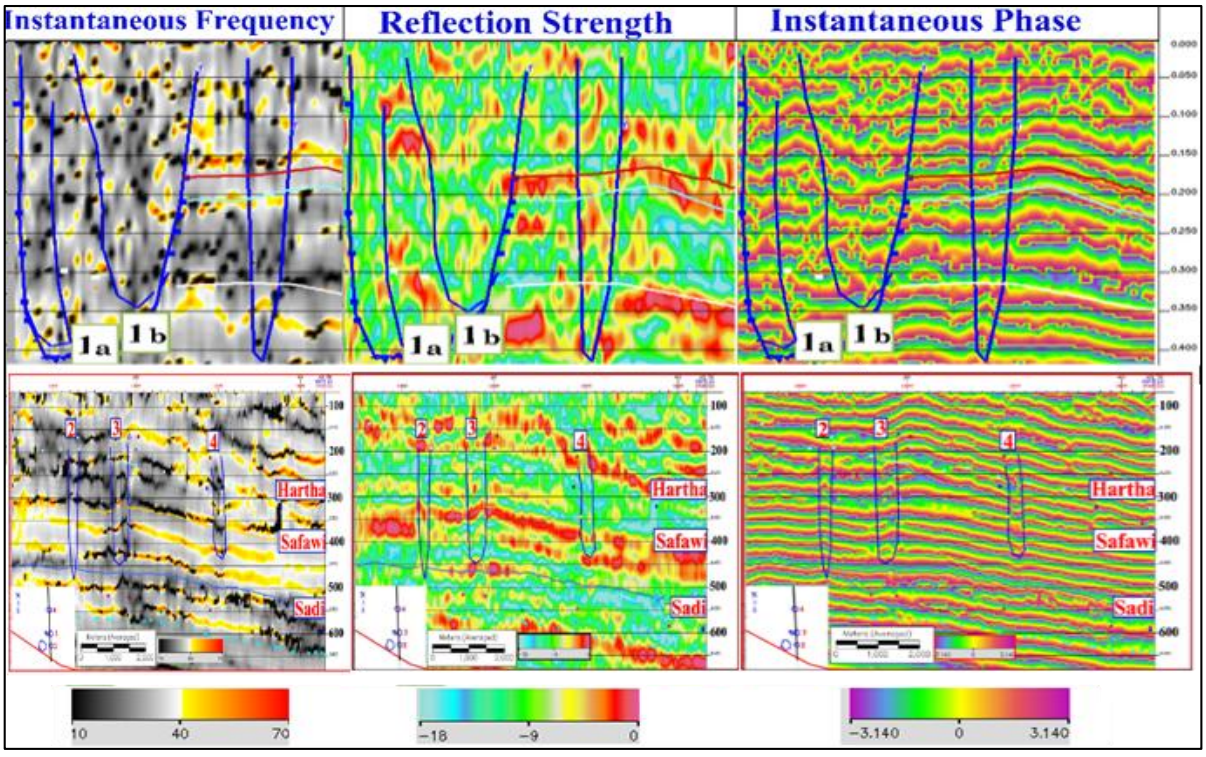

Figure 10. An example of seismic instantaneous frequency, seismic reflection strength, and seismic instantaneous phase of some karst features in the study area.

6. Conclusions

Daily, the seismic method proves its superiority in detecting subsurface subtle features such as karst. Cave and karst features represent corrosion in the sedimentary succession, which requires more skills to explore in the subsurface. Merjan 3D seismic volume is designed in high resolution with 380-fold and full 3D processing guarantees the data quality good enough for subsurface faults and karst mapping. Obvious lateral changes in seismic signature through the karst due to high lateral contrast in acoustic impedance along the karst. Variance seismic attributes are the perfect technique to distinguish the karst features. 35 locations of karst and fault systems have been determined. These results explained the mechanism of hydrocarbon leakage in the field and mobility system through the sedimentary succession from source to reservoir rocks. Seismic attributes (instantaneous frequency, instantaneous phase, and reflection magnitude) and seismic inversions have confirmed the presence of anomalies in physical properties through the karst relative to surrounding rocks. The presence of bitumen in the Wc-1 well indicates to leak of hydrocarbon to aquifers across the faults or karst features. Karst and associated fractures have an important impact on reservoir dynamic properties, where they may initially act as a conduit for fluid flow to enhance connectivity between the source and reservoir rocks, or enchantment the permeability system in the reservoir.

References

Al-Ameri, T. K., Al-Marsoumi, S. W., & Al-Musawi, F. A. (2015). Crude oil characterization, molecular affinity, and migration pathways of Halfaya oil field in Mesan Governorate, South Iraq. *Arabian Journal of Geosciences*, *8*(9), 7041–7058. https://doi.org/10.1007/s12517-014-1733-z

Al-Kadhimi, J.M.A., Sissakian, V.K., Fattah, A.S. and Deikran, D. B. (1996). *Tectonic Map of Iraq, scale 1: 1000 000, 2nd edit., GEOSURV, Baghdad, Iraq.*

Bown, T. D. (2011). *Legacy Seismic Investigations of Karst Surfaces: Implications for Heavy Oil Extraction From the Devonian Grosmont Formation, Northeastern Alberta, Canada*.

Burberry, C. M., Jackson, C. A. L., & Chandler, S. R. (2016). Seismic reflection imaging of karst in the Persian Gulf: Implications for the characterization of carbonate reservoirs. *AAPG Bulletin*, *100*(10), 1561–1584. https://doi.org/10.1306/04151615115

Eberli, G. P., Masaferro, J. L., & Sarg, J. F. (2005). Seismic imaging of carbonate reservoirs and systems. *AAPG Memoir*, *81*, 1–9. https://doi.org/10.1306/m81928

Ebuna, D. R., Kluesner, J. W., Cunningham, K. J., & Edwards, J. H. (2018). Statistical approach to neural network imaging of karst systems in 3D seismic reflection data. *Interpretation*, *6*(3), B15–B35. https://doi.org/10.1190/INT-2017-0197.1

El-Emam, A., Ebaid, A., Zahran, W., Al-Ajmi, B., Saleh, T., Cunnell, C., Laake, A., El Din, R. S., & Wahab, H. A. (2013). Delineation of karsts, a new approach using seismic attributes - Case study from Kuwait. *Society of Exploration Geophysicists International Exposition and 83rd Annual Meeting, SEG 2013: Expanding Geophysical Frontiers*, *September*, 3846–3850. https://doi.org/10.1190/segam2013-0927.1

Esker, D., Eberli, G. P., & McNeill, D. F. (1998). The structural and sedimentological controls on the reoccupation of quaternary incised valleys, Belize southern lagoon. *AAPG Bulletin*, *82*(11), 2075–2109. https://doi.org/10.1306/00aa7be4-1730-11d7-8645000102c1865d

Fisher, G., Hunt, D., Colpaert, A., G. Wall, B., & Henderson, J. (2020). *Comprehensive Karst Delineation from 3D Seismic Data*. https://doi.org/10.3997/2214-4609-pdb.248.293

Ford, D. (2007). Jovan Cvijić and the founding of karst geomorphology. *Environmental Geology*, *51*(5), 675–684. https://doi.org/10.1007/s00254-006-0379-x

Moldovanyi, E. P., Wall, F. M., & Zhang Jun Yan. (1995). Regional exposure events and platform evolution of Zhujiang Formation carbonates, Pearl River mouth basin: evidence from primary and diagenetic seismic facies. *Unconformities and Porosity in Carbonate Strata*, *63*, 125–140.

Rafaelsen, B., Elvebakk, G., Andreassen, K., Stemmerik, L., Colpaert, A., & Samuelsberg, T. J. (2008). From detached to attached carbonate buildup complexes - 3D seismic data from the upper Palaeozoic, Finnmark Platform, southwestern Barents Sea. *Sedimentary Geology*, *206*(1–4), 17–32. https://doi.org/10.1016/j.sedgeo.2008.03.001

Singh A., Sibam Chakraborty, S. A. (2010). Delineating Karst features using Advanced Interpretation. *8th Biennial International Conference & Exposition on Petroleum Geophysics*, 152.

Vahrenkamp, V. C., David, F., Duijndam, P., Newall, M., & Crevello, P. (2005). Growth architecture, faulting, and karstification of a middle Miocene carbonate platform, Luconia Province, offshore Sarawak, Malaysia. *AAPG Memoir*, *81*, 329–350. https://doi.org/10.1306/3fef4efb-1741-11d7-8645000102c1865d

Virs, R. (2015). *A comparative seismic study of gas chimney structures from active and dormant seepage sites offshore mid-Norway and west-Svalbard*. *May*.

Waltham, A. C., & Fookes, P. G. (2003). Engineering classification of karst ground conditions. *Quarterly Journal of Engineering Geology and Hydrogeology*, *36*(2), 101–118. https://doi.org/10.1144/1470-9236/2002-33

Zuo, J. P., Peng, S. P., Li, Y. J., Chen, Z. H., & Xie, H. P. (2009). Investigation of karst collapse based on 3-D seismic technique and DDA method at Xieqiao coal mine, China. *International Journal of Coal Geology*, *78*(4), 276–287. https://doi.org/10.1016/j.coal.2009.02.003

About the author

Dr. Ali M. Al-Rahim earned his B.Sc., M.Sc., and Ph.D. degrees in Geology-Geophysics from the University of Baghdad, Iraq. He has engaged in his academic career by teaching at the University of Baghdad since 2005. In 2016, he obtained the scientific title "Professor of Geophysics". He has published more than 60 scientific papers, published in local and international journals, mainly on Geophysical applications and Machine learning. He supervised several M.Sc. and Ph.D. students in the Department of Geology. His main interests are Computational Applications in Geophysics.

e-mail: ali.m@sc.uobaghdad.edu.iq